Journal Pre-proofs

A graphitized expanded graphite cathode for aluminum-ion battery with excellent rate capability

Xiaozhong Dong, Hao Chen, Haiwen Lai, Liyong Wang, Jiaqing Wang, Wenzhang Fang, Chao Gao

PII: S2095-4956(21)00406-X
DOI: https://doi.org/10.1016/j.jechem.2021.07.016
Reference: JECHEM 2063

To appear in: *Journal of Energy Chemistry*

Received Date: 27 December 2020
Revised Date: 2 July 2021
Accepted Date: 21 July 2021

Please cite this article as: X. Dong, H. Chen, H. Lai, L. Wang, J. Wang, W. Fang, C. Gao, A graphitized expanded graphite cathode for aluminum-ion battery with excellent rate capability, *Journal of Energy Chemistry* (2021), doi: https://doi.org/10.1016/j.jechem.2021.07.016

A graphitized expanded graphite cathode for aluminum-ion battery with excellent rate capability

Xiaozhong Dong[a,b], Hao Chen[a,*], Haiwen Lai[c], Liyong Wang[d], Jiaqing Wang[a], Wenzhang Fang[a], Chao Gao[a,*]

[a] *MOE Key Laboratory of Macromolecular Synthesis and Functionalization, Department of Polymer Science and Engineering, Key Laboratory of Adsorption and Separation Materials & Technologies of Zhejiang Province, Zhejiang University, Hangzhou 310027, Zhejiang, China*
[b] *Department of Materials Engineering, Taiyuan Institute of Technology, Taiyuan 030008, Shanxi, China*
[c] *Hangzhou Gaoxi Technology Co. Ltd., Hangzhou 310000, Zhejiang, China*
[d] *Hebei Normal University for Nationalities, Chengde 067000, Hebei, China*

***Corresponding author**.
E-mail addresses: chaogao@zju.edu.cn (C. Gao), chenhao_chem@163.com (H. Chen)

ABSTRACT

Aluminum-ion battery (AIB) is very promising for its safety and large current charge-discharge. However, it is challenging to build a high-performance AIB system based on low-cost materials especially cathode & electrolyte. Despite the low-cost expanded graphite-triethylaminehydrochloride (EG-ET) system has been improved in cycle performance, its rate capability still remains a gap with the expensive graphene-alkylimidazoliumchloride AIB system. In this work, we treated the cheap EG appropriately through an industrial high-temperature process, employed the obtained EG3K (treated at 3000 °C) cathode with $AlCl_3$-ET electrolyte, and built a novel, high-rate capability and double-cheap AIB system. The new EG3K-ET system achieved the cathode capacity of average 110 mAh g^{-1} at 1 A g^{-1} with 18000 cycles, and retained the cathode capacity of 100 mAh g^{-1} at 5 A g^{-1} with 27500 cycles (fast charging of 72 s). Impressively, we demonstrated that a battery pack (EG3K-ET system, 12 mAh) had successfully driven the Model car running 100 m long. In

addition, it was confirmed that the improvement of rate capability in the EG3K-ET system was mainly derived by deposition, and its capacity contribution ratio was about 53.7%. This work further promoted the application potential of the low-cost EG-ET AIB system.

Keywords: Aluminum-ion battery; Expanded graphite; Triethylamine hydrochloride

1. Introduction

Aluminum-ion battery (AIB) is a novel rechargeable battery, employing the ionic liquid electrolyte and the reversible $Al_2Cl_7^-$|Al pair reaction, which gives AIB with outstanding advantages in terms of safety and large current charge-discharge. Relative to the theory capacity of aluminum anode (2978 mAh g^{-1} and 8034 mAh cm^{-3}), the AIB cathode capacity becomes a major limiting factor and bottleneck that hurdles it practical applications. As for AIB cathode materials, the conversion-type chalcogenide materials (SnS_2 [1], CoS_2 [2], $CoSe_2$ [3], CuS [4], $Cu_{2-x}Se$ [5], MXene-Se [6], TiO_2@Se [7], MOFs [8] and Mo_6S_8 [9]) exhibited high capacities but fast fading; while the intercalation-type graphite materials (graphite foam [10–12], pyrolytic graphite [13–15], natural graphite [16–21], expanded graphite [22,23] and graphene [24–31]) displayed stable capacities and super long cycling. The graphene cathode has achieved a super high rate capability (117 mAh g^{-1} at 5 A g^{-1}) and super long cycle life (250000 cycles), yet relatively high-cost derived from the full exfoliation of graphite sheets [26]. Meanwhile, the cheap and un-exfoliated graphite cathode (pyrolytic graphite and natural graphite) only gave the capacity of 60 mAh g^{-1}. Obviously, there is a contradiction between the high-performance and the price of AIB cathode materials. Additionally, the $AlCl_3$-alkylimidazoliumchloride (EMI) electrolyte [10,11,16,24,26] was the most studied, the best performing, but also extremely expensive. In addition, some kinds of cheap electrolytes have been

developed, including $AlCl_3$-urea electrolyte [32], $AlCl_3$-NaCl electrolyte [33,34], $AlCl_3$-NaCl-KCl electrolyte [35] and $AlCl_3$-acetamide electrolyte [36], but with low Coulombic efficiency (CE) and insufficient cycle life. Therefore, it is challenging to obtain a high-performance and double-cheap AIB system that is limited by both cathode and electrolyte. In our previous work, a double-cheap AIB system was obtained, consisting of commercial expanded graphite (EG) cathode and $AlCl_3$-triethylaminehydrochloride (ET) electrolyte [22]. Despite its price is lower, and its performance (78.3 mAh g^{-1} at 5 A g^{-1} with 77.5% retention after 30000 cycles) is better than most graphite-EMI system, there still remains a gap with the above-mentioned graphene-EMI system [26].

In this work, we treated the cheap EG appropriately through an industrial high temperature furnace. The obtained EG3K cathode was combined with $AlCl_3$-ET electrolyte, and a high-rate capability and double-cheap AIB system was built. The novel EG3K-ET system had a significant improvement in rate capability, reaching the capacity of 108.9 ± 0.5 mAh g^{-1} at 1 A g^{-1} and 98.0 ± 4.4 mAh g^{-1} at 5 A g^{-1}, close to the performance of the graphene-EMI system. Especially, we demonstrated that the battery pack (EG3K-ET system, 12 mAh) had driven the Model car running 100 m long. Besides, the improvement of rate capability in the EG3K-ET system was mainly contributed by deposition, the precipitates very likely come from $AlCl_4^-$ ion containing electrolyte as they shared similar chemical composition, and the deposition capacity contribution ratio was about 53.7%. In one word, this work further promoted the application potential of the low-cost EG-ET AIB system.

2. Experimental

2.1. Preparation of the EG3K cathode film

The wormlike EG (Hangzhou Gaoxi Technology Co. Ltd., China) was annealed at 3000 °C to obtain EG3K, through an industrial high temperature furnace (Zhuzhou Jinrui induction furnace, China). Then, the free-standing EG3K cathode film was prepared by direct compressing [22], with area loading of 2 mg cm^{-2}. Furthermore, the EG3K powder/PVDF (mass ratio of 9/1) composite cathode film was prepared by coating method [37], with area loading of 3 mg cm^{-2}.

2.2. Material characterization

EG3K and the free-standing EG3K cathode film were characterized by scanning electron microscope (SEM, Hitachi S4800), transmission electron microscope (TEM, JEM-2100), X-ray diffractormeter (XRD, BRUKER D8), Raman (RENISHAW inVia-Reflex) and surface area & porosity analyzer (ASAP 2020 HD88). The EG3K cathode film by coating method was characterized by energy dispersive X-ray spectroscopy (EDS, ZEISS EVO18) and another XRD (BRUKER D8).

2.3. Battery assembly

In the Ar-filled glovebox (O_2 < 0.1 ppm, H_2O < 0.1 ppm), the CR2025 coin cell was assembled with the EG3K film (circular electrode, diameter/1 cm) as the working electrode, aluminum foil (thickness/20 μm) as the counter and reference electrode, the $AlCl_3$-ET (mole ratio of 1.5/1) mixture as the electrolyte, and glass fibre membrane (Whatman 934-AH) as the separator. The used $AlCl_3$-ET electrolyte was prepared by the references [22,27]. The pouch cell for AIB demonstration was assembled with a 5 cm ×8 cm free-standing EG3K cathode film (area loading of 3.5 mg cm^{-2}).

2.4. Electrochemical measurement

The cycling performance and rate capability of AIB coin cells were conducted on a battery test system (LAND CT2001A). The cutoff voltage range was 0.70–2.54 V. The cyclic voltammetry (CV) curve was obtained at 1 mV s^{-1} on an electrochemical

workstation (Chenhua CHI660E). The electrochemical impedance spectroscopy (EIS) was recorded from 10^5 to 0.01 Hz on the same workstation.

3. Results and discussion

3.1. Characterization of the EG3K material

After treating at 3000 °C, EG3K kept negligible oxygen heteroatoms (Fig. S1). Benefiting from the rearrangement of defective hexatomic carbon rings, EG3K has smoother curved surfaces (Fig. 1a) and its graphite sheets with fewer defects (Fig. 1e, I_D/I_G=0.0409), relative to commercial EG (Fig. S2). Significantly, the graphite sheet edges fused (arrows in Fig. 1b and c) and graphite sheets were more regular. Whereas, the interlayer space is almost no change, which reflected by C (002) peak at 2θ = 26.42° (Fig. 1d). EG3K inherited the hierarchical pore structure (3 and 40 nm) and large BET special surface area of 46.07 m^2 g^{-1} (Fig. 1f), which are beneficial to enhance the diffusion rate of $AlCl_4^-$ ions [14,15] and the AIB capacity contributed by $AlCl_4^-$ deposition [22], thus increasing its rate capability.

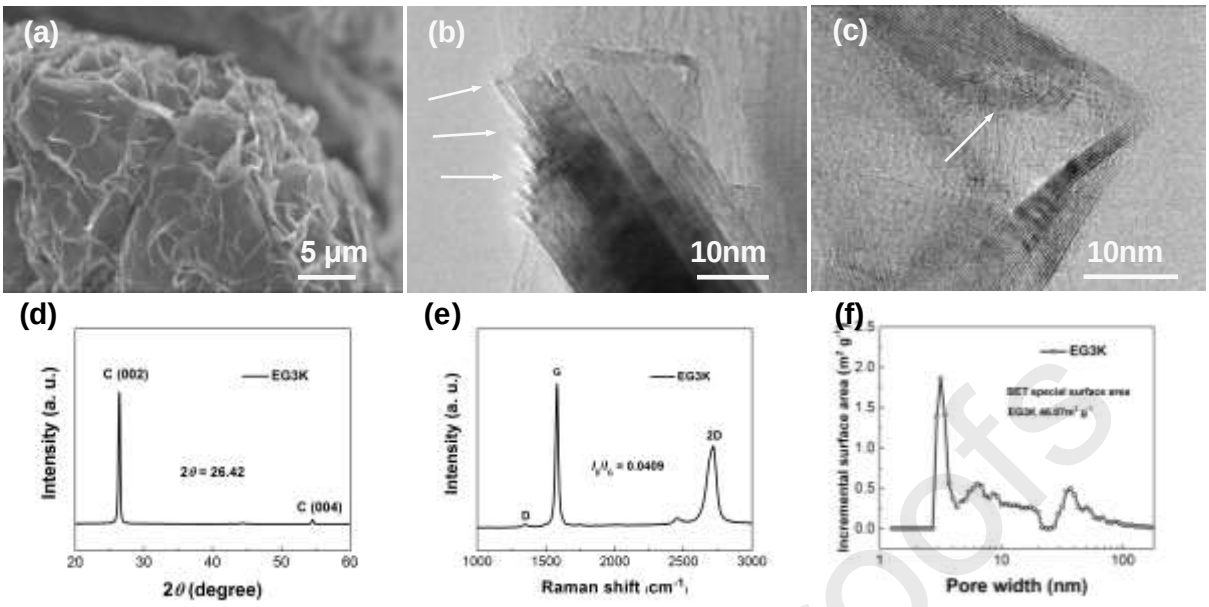

Fig. 1. Material characterization of EG3K. (a) SEM image; (b and c) TEM images; (d) XRD pattern; (e) Raman spectra; (f) pore diameter distribution curve measured by nitrogen adsorption method.

3.2. Electrochemical performance of the EG3K cathode

As mentioned, the double-cheap EG-ET AIB system has been achieved with the cathode capacity of 78.3 mAh g^{-1} at 5 A g^{-1} and 77.5% capacity retention after 30000 cycles. But, its rate capability is not good enough relative to the graphene-EMI system. Here we employed the free-standing EG3K cathode film with fewer defects based on the EG-ET system.

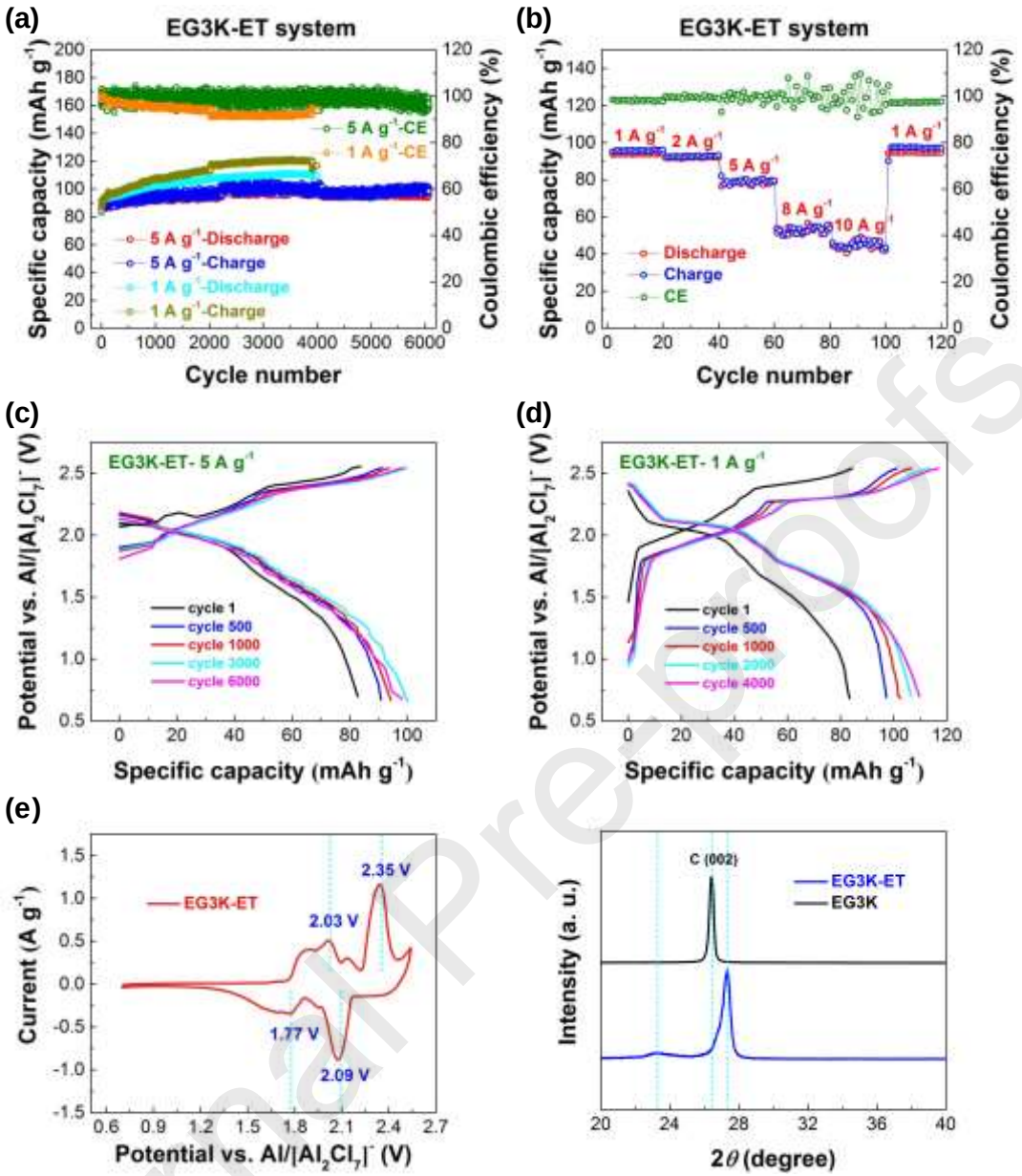

Fig. 2. Electrochemical performance of the EG3K-ET AIB system with the free-standing cathode film (area loading of 2 mg cm^{-2}). (a) Cycling performance at 1 A g^{-1} and 5 A g^{-1}; (b) rate capability; (c and d) voltage-capacity curves at 5 A g^{-1} and 1 A g^{-1}; (e) CV curve scanned at 1 mV s^{-1}; (f) *ex situ* XRD pattern of EG3K cathode film at the fully charged state. The cutoff voltage range is 0.7–2.54 V.

As shown in Fig. 2(a), at the current density of 1 A g^{-1}, the cathode capacity of EG3K-ET AIB system reached 108.9 ± 0.5 mAh g^{-1}, which increased by 10.4% than EG-ET system (Fig. S3a and Table S1), yet with lower CE of 91.9% ± 0.7% and shorter life of 4000 cycles. This is due to that the perfect graphite sheets in EG3K can provide more locations of $AlCl_4^-$ deposition, including fusion sites of graphite sheets as shown in Fig. 1(c). Meanwhile, EG3K has a stiffness enhancement after high temperature treatment, and reduces the self-adhesion, leading to the easy cracking of the electrode and short cycling life.

When the charge-discharge rate increased to 5 A g^{-1} (~50 C), the cathode capacity of EG3K-ET system improved 25.1% (Fig. S3b and Table S1) and delivered 98.0 ± 4.4 mAh g^{-1} with 6000 cycles. Corresponding to this, the EG3K-ET AIB system exhibited excellent rate capability (Figs. 2b and S3c). All these supported that the high-quality graphitized carbon material could improve the cathode capacity of AIB. As indicated from EIS results (Fig. S4), the EG3K-ET AIB system possessed lower internal resistance and faster diffusion rate of $AlCl_4^-$.

Fig. 2(d) displayed the initial increase and stable cycling of battery capacity, which reflected the continuous exfoliation to EG3K graphite sheets induced by $AlCl_4^-$ intercalation [11,22,38,39]. At 1 A g^{-1}, the EG3K-ET system exhibited two obvious charge platforms of 2.0 and 2.2 V, and two corresponding discharge platforms of 1.7 and 2.1 V. This is consistent with its CV curve in Fig. 2(e).

It has been confirmed that the high capacity of EG-ET system was contributed by $AlCl_4^-$ deposition and its stage 4 intercalation [22], as shown in Fig. S5. We also noticed that the CV curve of EG3K-ET system was almost the same with EG-ET system (Fig. S3d). It means that the EG3K-ET AIB system had roughly the same operating mechanism. The difference is that, at the fully charged state (Fig. 2f), the

C(002) peak of EG3K at 2θ = 26.42° (d = 0.3371 nm) split into two peaks at 2θ = 23.28° (d_1 = 0.3818 nm) and 27.32° (d_2 = 0.3262 nm), and the corresponding d_1/d_2 is 1.17, consistent with the stage 5 intercalation of $AlCl_4^-$[40]. The stage 5 intercalation only afforded the cathode capacity of 50 mAh g^{-1} for AIB [40], however, the EG3K-ET system exhibited much higher capacity. Therefore, in the EG3K-ET AIB system, the capacity improvement by graphitization was mostly from the contribution by $AlCl_4^-$ deposition proposed in our previous work [22]. Especially, at the large current of 5 A g^{-1} (~50 C), the time for $AlCl_4^-$ intercalation reduced, and the contribution of $AlCl_4^-$ deposition became more obvious. As indicated in Fig. 2(c), charge-discharge platforms of EG3K-ET system were not very clear at 5 A g^{-1}.

3.3. Operating mechanism of the EG3K-ET AIB system

The $AlCl_4^-$ intercalation mechanism for AIB has been proved generally by *ex situ* XRD patterns [10,16,22], showing the stage 4 $AlCl_4^-$ intercalation in the EG-ET system [22] while stage 5 for the EG3K-ET system. The $AlCl_4^-$ deposition mechanism is another important component for charge storage of EG-based cathode materials with high special surface area.

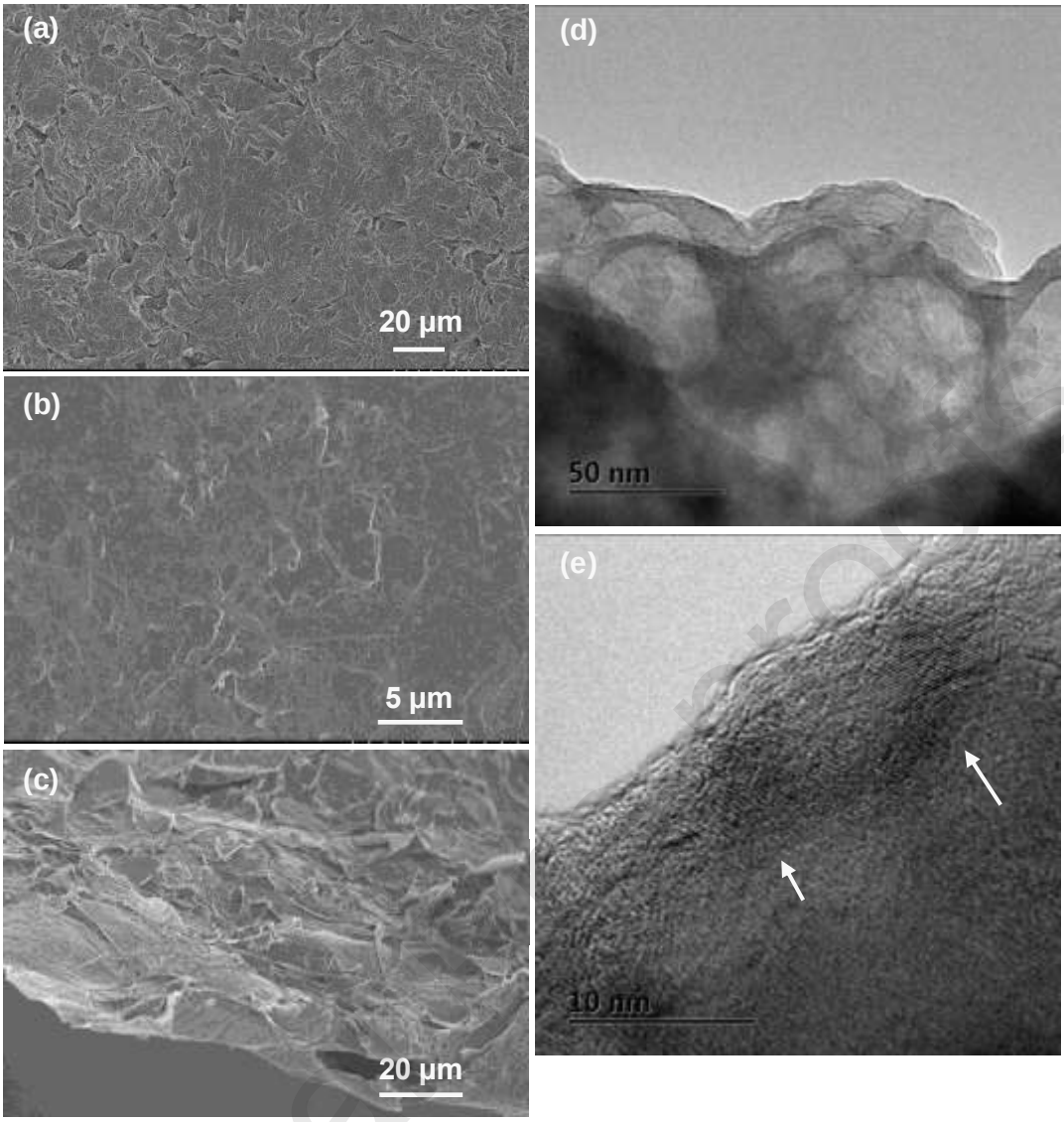

Fig. 3. (a) SEM image of the original EG3K free-standing film; (b and c) surface and cross-section SEM images of the free-standing EG3K cathode film at the fully charged state (2.54 V); (d and e) TEM images of the EG3K cathode material at the fully charged state (2.54 V).

As shown in Fig. 3(a), many wrinkles existed on the surface of the original EG3K free-standing film. At the fully charged state, there formed a thick and homogeneous layer by $AlCl_4^-$ deposition on the surface of EG3K cathode film (Fig. 3b). The cross-section image (Fig. 3c) presented that the $AlCl_3$-ET electrolyte was well

infiltrated in the EG3K material, and $AlCl_4^-$ deposition also took place in the interior of the EG3K cathode. The TEM image in Fig. 3(d) also showed that nanoscale hollow cavities existed ubiquitously at the fully charged state. As shown in Fig. 3(e), the cavity wall was composed of graphite sheets. Thus, the locations of $AlCl_4^-$ deposition included the surface of the EG3K electrode, nanoscale hollow cavities and fusion sites of graphite sheets.

The EG3K-ET AIB system exhibited higher capacity and better rate capability than EG-ET system, but the $AlCl_4^-$ intercalation ability (stage 5) declined. It is most likely that EG3K possessed more perfect graphite sheets and more deposition sites, and excessive $AlCl_4^-$ deposition limited $AlCl_4^-$ intercalation in the EG3K-ET system. Therefore, the improvement of AIB capacity and rate capability by graphitization, mainly derived from the contribution of $AlCl_4^-$ deposition.

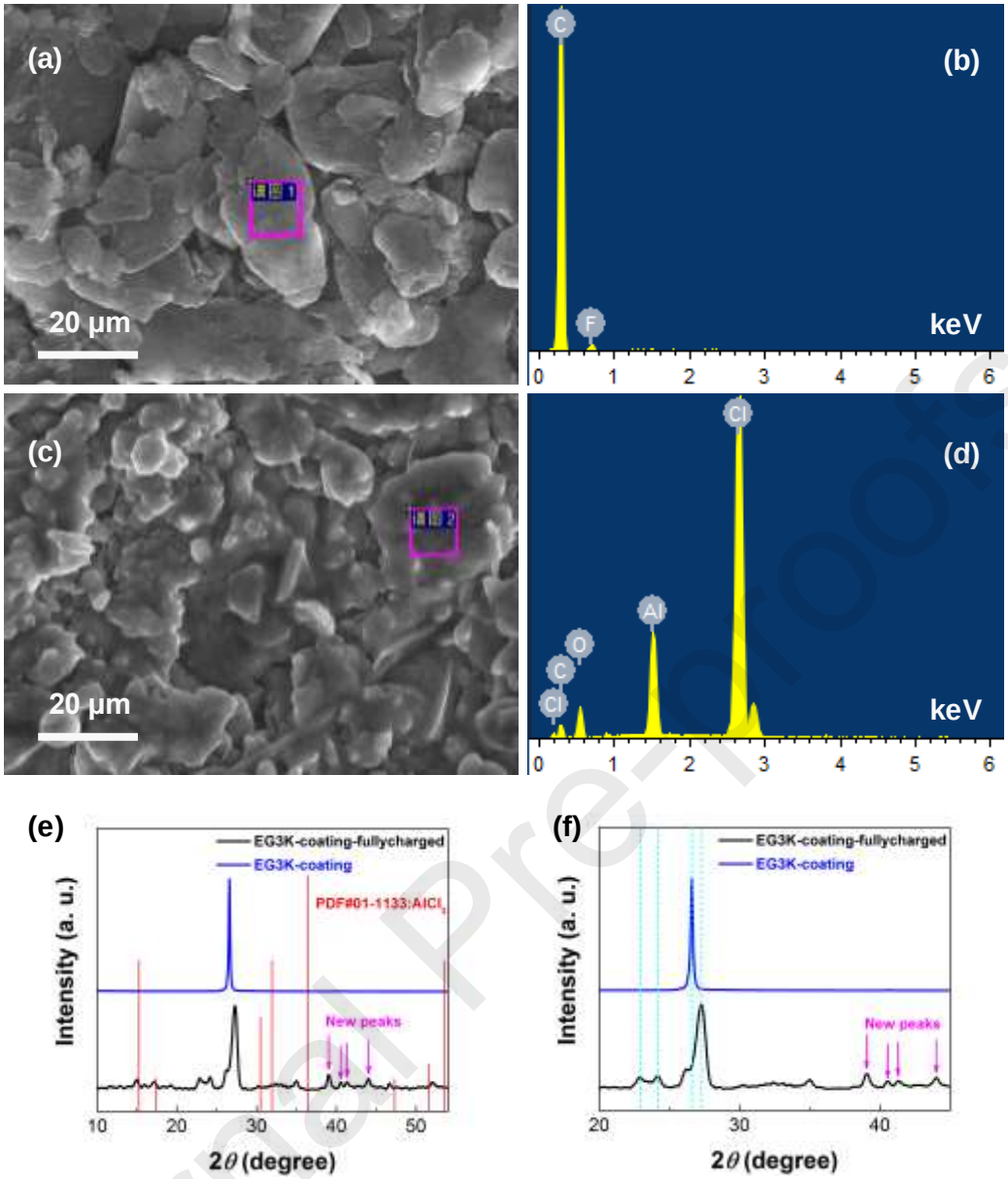

Fig. 4. (a and b) Surface EDS results of the original EG3K coating film; (c and d) surface EDS results of the EG3K coating cathode at the fully charged state (2.54 V); (e and f) *ex situ* XRD patterns of the EG3K coating cathode at the fully charged state (2.54 V).

Table 1. The EDS element content from Fig. 4 (b and d).

	EG3K-coating		EG3K-coating-fullycharged	
Element	Wt%	At%	Wt%	At%
C	94.59	96.51	33.33	50.65
F	5.41	3.49	–	–
O	–	–	22.10	25.22
Al	–	–	7.30	4.94
Cl	–	–	37.26	19.19

To further ascertain the deposition mechanism and its capacity contribution, the surface EDS analysis was conducted with the EG3K coating cathode at the fully charged state (2.54 V). The original EG3K coating film has a surface composition of 96.51 at% C and 3.49 at% F, as shown in Fig. 4 (a and b) and Table 1. While fully charged, the surface deposit (Fig. 4c) include 4.94 at% Al and 19.19 at% Cl, and the atom ratio of Cl/Al is 3.88 (Fig. 4d and Table 1). This reflected that the precipitates very likely come from $AlCl_4^-$ ion containing electrolyte as they shared similar chemical composition, and the deposition existed on the surface of EG3K cathode at the fully charged state. Referring to C content of 50.65 at% in Table 1, the atom ratio of C/Al is about 10 on the surface of EG3K cathode at the fully charged state, which means, on the electrode surface with the fully charged state, ten C atoms combine with one Al atom. The EG3K-ET AIB system exhibited the capacity of 108 mAh g^{-1} at 1 A g^{-1} (Fig. 2a), and its stage 5 intercalation (Fig. 2f) had the theory capacity of 50 mAh g^{-1} [40] at the fully charged state. Therefore, the deposition capacity contribution ratio was about (108−50)/108 = 53.7% from $AlCl_4^-$ deposition.

Ex situ XRD was also conducted with the EG3K coating cathode at the fully charged state (2.54 V). Besides the split of C(002) peak, new peaks at 2θ = 39.06°,

40.56°, 41.31° and 44.01° were also observed (Fig. 4e). These new peaks emerged at the fully charged state, neither belong to $AlCl_3$ (PDF#01-1133, Fig. 4e) nor ET (PDF#38-1974, Fig. S6). This further supported that the precipitates had similar chemical composition with $AlCl_4^-$, which existed on the surface of EG3K cathode at the fully charged state. In Fig. 4(f), the first group of split peaks of the C(002) peak were 2θ = 22.89° (d_1 = 0.3882 nm) and 27.27° (d_2 = 0.3268 nm), and the corresponding d_1/d_2 is 1.19, consistent with the stage 5 intercalation of $AlCl_4^-$ [40]. The second group of split peaks were 2θ = 24.17° (d_1 = 0.3679 nm) and 27.27° (d_2 = 0.3268 nm), and the corresponding d_1/d_2 is 1.13, consistent with the stage 6 intercalation of $AlCl_4^-$ [40]. That means stages 5 & 6 intercalation of $AlCl_4^-$ existed in the EG3K-ET AIB system, consist with results of the EG3K free-standing film at the fully charged state.

3.4. Electrochemical performance of the EG3K-coating cathode

To demonstrate the excellent rate capability of the EG3K-ET AIB system, we assembled the pouch cell with a 5 cm ×8 cm free-standing EG3K film. Two pouch cells were connected in series. The battery pack with 12 mAh drove the Model car running 100 m long (Fig. 5a), as shown in the supplementary video. After then, the output voltage of used pouch cell still retained 2.0 V (Fig. 5b).

We also noticed that the EG3K free-standing cathode improved the rate capability, yet its cycling life reduced due to the decrease of self-adhesion. Furthermore, we used PVDF as binder, the EG3K powder/PVDF (mass ratio of 9/1) coating film as cathode to increase the cycling life of EG3K AIB. As shown in Fig. 5(c), the EG3K-ET-coating system reached the cathode capacity of 128 mAh g^{-1} of the maximum value, and 110 mAh g^{-1} of the average value at 1 A g^{-1} with 18000 cycles. At 5 A g^{-1} (Fig. 5d and Table S1), the EG3K-ET-coating system retained the cathode

capacity of 100 mAh g^{-1} with 27500 cycles. The EG3K coating cathode further improved the cycling performance of the EG3K-ET system.

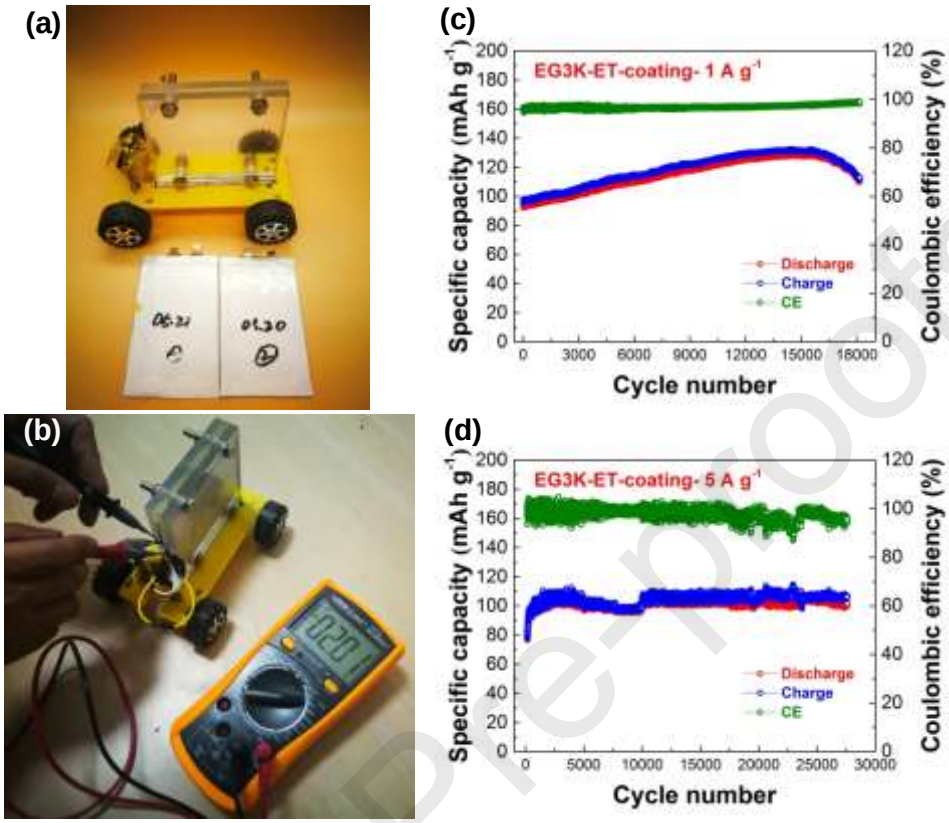

Fig. 5. (a) the Model car and two pouch cells used for AIB demonstration; (b) the monomer residual voltage of 2.0 V after 100-m driving; (c and d) cycling performance at 1 A g^{-1} and 5 A g^{-1} of the EG3K-ET-coating AIB system. The used coating cathode is an EG3K powder/PVDF (mass ratio of 9/1) composite film with area loading of 3 mg cm^{-2}. The cutoff voltage range is 0.7–2.54 V.

4. Conclusions

In summary, we employed the graphitized EG3K cathode and $AlCl_3$-ET electrolyte to enhance the rate capability of EG-based AIB system. By using the graphitized cathode, the EG3K-ET AIB system reached the capacity of average110 mAh g^{-1} at 1 A g^{-1} with 18000 cycles, and retained the capacity of 100 mAh g^{-1} with 27500 cycles at 5 A g^{-1}. Besides, the improvement of AIB capacity and rate capability by

graphitization was mainly derived from the contribution by deposition, the precipitates very likely come from $AlCl_4^-$ ion containing electrolyte as they shared similar chemical composition, and the deposition capacity contribution ratio was about 53.7%. This work further promoted the application potential of the double-cheap EG-ET AIB system.

Declaration of Competing Interest

The authors declare that they have no known competing financial interests or personal relationships that could have appeared to influence the work reported in this paper.

Acknowledgements

The authors would like to acknowledge the support of the National Natural Science Foundation of China (51533008, 51703194 and 21805242), the National Key R&D Program of China (2016YFA0200200), and the Excellent Postdoctoral Special Fund of Zhejiang University for funding this research work.

Supplementary materials

Supplementary material associated with this article can be found, in the online version, at doi:

References

[1] Y.X. Hu, B. Luo, D.L. Ye, X.B. Zhu, M.Q. Lyu, L.Z. Wang, Adv. Mater. 29 (2017) 1606132.

[2] Y.X. Hu, D.L. Ye, B. Luo, H. Hu, X.B. Zhu, S.C. Wang, L.L. Li, S.J. Peng, L.Z. Wang, Adv. Mater. 30 (2018) 1703824.

[3] T.H. Cai, L.M. Zhao, H.Y. Hu, T.G. Li, X.C. Li, S. Guo, Y.P. Li, Q.Z. Xue, W. Xing, Z.F. Yan, L.Z. Wang, Energy Environ. Sci. 11 (2018) 2341-2347.

[4] S. Wang, S.Q. Jiao, J.X. Wang, H.S. Chen, D.H. Tian, H.P. Lei, D.N. Fang, ACS Nano 11 (2017) 469-477.

[5] J.L. Jiang, H. Li, T. Fu, B.J. Hwang, X. Li, J.B. Zhao, ACS Appl. Mater. Interfaces 10 (2018) 17942-17949.

[6] Z. Li, X. Wang, W. Zhang, S. Yang, Chem. Eng. J. 398 (2020) 125679.

[7] Z. Li, X. Wang, X. Li, W. Zhang, Chem. Eng. J. 400 (2020) 126000.

[8] S. Zheng, Q. Li, H. Xue, H. Pang, Q. Xu, Natl. Sci. Rev. 7 (2019) 305-314.

[9] L.X. Geng, G.C. Lv, X.B. Xing, J.C. Guo, Chem. Mater. 27 (2015) 4926-4929.

[10] M.C. Lin, M. Gong, B. Lu, Y. Wu, D.Y. Wang, M. Guan, M. Angell, C. Chen, J. Yang, B.J. Hwang, H. Dai, Nature 520 (2015) 325-328.

[11] Y. Wu, M. Gong, M.C. Lin, C. Yuan, M. Angell, L. Huang, D.Y. Wang, X. Zhang, J. Yang, B.J. Hwang, H. Dai, Adv. Mater. 28 (2016) 9218-9222.

[12] Y. Feng, S. Chen, J. Wang, B. Lu, J. Energy Chem. 43 (2020) 129-138.

[13] G.A. Elia, I. Hasa, G. Greco, T. Diemant, K. Marquardt, K. Hoeppner, R.J. Behm, A. Hoell, S. Passerini, R. Hahn, J. Mater. Chem. A 5 (2017) 9682-9690.

[14] N.P. Stadie, S.T. Wang, K.V. Kraychyk, M.V. Kovalenko, ACS Nano 11 (2017) 1911-1919.

[15] Z.A. Zafar, S. Imtiaz, R. Li, J. Zhang, R. Razaq, Y. Xin, Q. Li, Z. Zhang, Y. Huang, Solid State Ion. 320 (2018) 70-75.

[16] D.Y. Wang, C.Y. Wei, M.C. Lin, C.J. Pan, H.L. Chou, H.A. Chen, M. Gong, Y. Wu, C. Yuan, M. Angell, Y.J. Hsieh, Y.H. Chen, C.Y. Wen, C.W. Chen, B.J. Hwang, C.C. Chen, H. Dai, Nat. Commun. 8 (2017) 14283.

[17] G. Wang, M. Yu, J. Wang, D. Li, D. Tan, M. Loeffler, X. Zhuang, K. Muellen, X. Feng, Adv. Mater. 30 (2018) 1800533.

[18] H. Sun, W. Wang, Z. Yu, Y. Yuan, S. Wang, S. Jiao, Chem. Commun. 51 (2015) 11892-11895.

[19] S.Q. Jiao, H.P. Lei, J.G. Tu, J. Zhu, J.X. Wang, X.H. Mao, Carbon 109 (2016) 276-281.

[20] K.V. Kraychyk, S. Wang, L. Piveteau, M.V. Koyalenko, Chem. Mater. 29 (2017) 4484-4492.

[21] S.T. Wang, K.V. Kravchyk, F. Krumeich, M.V. Kovalenko, ACS Appl. Mater. Interfaces 9 (2017) 28478-28485.

[22] X. Dong, H. Xu, H. Chen, L. Wang, J. Wang, W. Fang, C. Chen, M. Salman, Z. Xu, C. Gao, Carbon 148 (2019) 134-140.

[23] Z. Li, J. Li, X. Li, W. Zhang, J. Power Sources 467 (2020) 228323.

[24] H. Chen, F. Guo, Y. Liu, T. Huang, B. Zheng, N. Ananth, Z. Xu, W. Gao, C. Gao, Adv. Mater. 29 (2017) 1605958.

[25] H. Chen, C. Chen, Y.J. Liu, X.L. Zhao, N. Ananth, B.N. Zheng, L. Peng, T.Q. Huang, W.W. Gao, C. Gao, Adv. Energy Mater. 7 (2017) 1700051.

[26] H. Chen, H. Xu, S. Wang, T. Huang, J. Xi, S. Cai, F. Guo, Z. Xu, W. Gao, C. Gao, Sci. Adv. 3 (2017) eaao7233.

[27] H. Xu, T. Bai, H. Chen, F. Guo, J. Xi, T. Huang, S. Cai, X. Chu, J. Ling, W. Gao, Z. Xu, C. Gao, Energy Storage Materials 17 (2018) 38-45.

[28] S.C. Jung, Y.J. Kang, D.J. Yoo, J.W. Choi, Y.K. Han, J. Phys. Chem. C 120 (2016) 13384-13389.

[29] Q. Zhang, L. Wang, J. Wang, C. Xing, J. Ge, L. Fan, Z. Liu, X. Lu, M. Wu, X. Yu, H. Zhang, B. Lu, Energy Storage Materials 15 (2018) 361-367.

[30] H. Ding, J. Zhou, A.M. Rao, B. Lu, Natil. Sci. Rev. 8 (2020) nwaa276.

[31] Q. Zhang, X. Cheng, C. Wang, A.M. Rao, B. Lu, Energy Environ. Sci. 14 (2021) 965-974.

[32] M. Angell, C.J. Pan, Y.M. Rong, C.Z. Yuan, M.C. Lin, B.J. Hwang, H.J. Dai, Proc. Natl. Acad. Sci. U. S. A. 114 (2017) 834-839.

[33] Y. Song, S.Q. Jiao, J.G. Tu, J.X. Wang, Y.J. Liu, H.D. Jiao, X.H. Mao, Z.C. Guo, D.J. Fray, J. Mater. Chem. A 5 (2017) 1282-1291.

[34] Z. Li, X. Li, W. Zhang, J. Power Sources 475 (2020) 228628.

[35] C.-Y. Chen, T. Tsuda, S. Kuwabata, C.L. Hussey, Chem. Commun. 54 (2018) 4164-4167.

[36] N. Canever, N. Bertrand, T. Nann, Chem. Commun. 54 (2018) 11725-11728.

[37] X.Z. Dong, C.X. Lu, L.Y. Wang, P.C. Zhou, D.H. Li, L. Wang, G.P. Wu, Y.H. Li, Rsc Adv. 6 (2016) 12737-12743.

[38] H.P. Lei, J.G. Tu, Z.J. Yu, S.Q. Jiao, ACS Appl. Mater. Interfaces 9 (2017) 36702-36707.

[39] J.Z. Wang, K.K. Manga, Q.L. Bao, K.P. Loh, J. Am. Chem. Soc. 133 (2011) 8888-8891.

[40] C.J. Pan, C.Z. Yuan, G.Z. Zhu, Q. Zhang, C.J. Huang, M.C. Lin, M. Angell, B.J. Hwang, P. Kaghazchi, H.J. Dai, Proc. Natl. Acad. Sci. U.S.A. 115 (2018) 5670-5675.

Graphical Abstract

A graphitized expanded graphite cathode has improved AIB rate capability, retained 100 mAh g^{-1} at 5 A g^{-1} with 27500 cycles (fast charging of 72 s), which was mainly derived from $AlCl_4^-$ deposition.

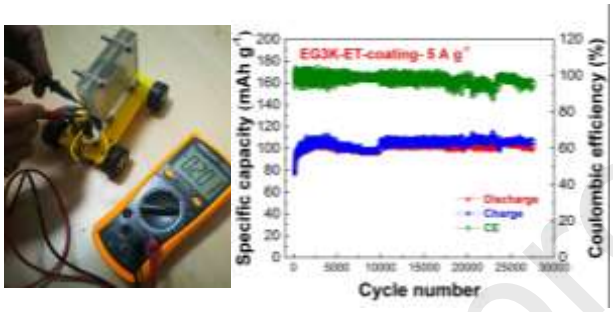

Graphical Abstract

A graphitized expanded graphite cathode has improved AIB rate capability, which was mainly derived from $AlCl_4^-$ deposition.

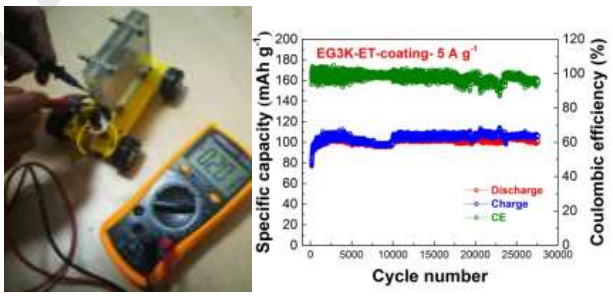

Dear editor:

Here within enclosed is our manuscript of **A graphitized expanded graphite cathode for aluminum-ion battery with excellent rate capability** for consideration to be published on "*Journal of Energy Chemistry*". No conflict of interest exits in the submission of this manuscript, and the manuscript is approved by all authors for publication. I would like to declare on behalf of my co-authors, that the work described is original research, not published previously, and not under consideration for publication elsewhere, in whole or in part.

The significance of our work:

Aluminum-ion battery (AIB) is very promising for its safety and large current charge-discharge. However, it is challenging to build a high-performance AIB system based on low-cost materials especially cathode & electrolyte. Despite the low-cost expanded graphite-triethylamine hydrochloride (EG-ET) system has been improved in cycle performance, its rate capability still remains a gap with the expensive graphene-alkylimidazolium chloride AIB system.

In this work, we treated the cheap EG appropriately through an industrial high-temperature process, employed the obtained EG3K (treated at 3000 °C) cathode with $AlCl_3$-ET electrolyte, and built a novel, high-rate capability and double-cheap AIB system. The new EG3K-ET system achieved the cathode capacity of average 110 mAh g^{-1} at 1 A g^{-1} with 18 000 cycles, and retained the cathode capacity of 100 mAh g^{-1} at 5 A g^{-1} with 27 500 cycles (fast charging of 72 seconds). Impressively, we demonstrated that a battery pack (EG3K-ET system, 12 mAh) had successfully driven the Model car running 100 meters long. In addition, it was confirmed that the improvement of rate capability in the EG3K-ET system was mainly derived by deposition, and its capacity contribution ratio was about 53.7%. This work further promoted the application potential of the low-cost EG-ET AIB system.

Thank you very much for consideration!

Yours sincerely,

Prof. Chao Gao